Coordination capacity of Keggin anions as polytopic ligands: case study of $[VNb_{12}O_{40}]^{15-}$

Anna A. Mukhacheva,[a] Victoria V. Volcheck,[a] Dmitry G. Sheven,[a] Vadim V. Yanshole,[b,c] Nikolay B. Kompankov,[a] Mohamed Haouas,[d] Pavel A. Abramov,*[a,e] and Maxim N. Sokolov [a]

Supporting information

Table of Contents

General information 3

Table S1. Experimental details 5

Table S2. Selected geometric parameters (Å) 6

Synthesis 10

Table S3. Atomic ratios Nb/V and Nb/Ru calculated from HPLC-ICP-AES-data 11

Fig. S1. ^{51}V NMR spectrum of $Na_9H_4[VNb_{12}O_{40}\{NbO(CO_3)\}_2]\cdot 34H_2O$ in D_2O 12

Fig. S2. ^{51}V NMR spectrum of $Na_5[\{(C_6H_6)Ru\}_5VNb_{12}O_{40}]\cdot 16H_2O$ in D_2O 12

Fig. S3. IR spectrum of $Na_5[\{(C_6H_6)Ru\}_5VNb_{12}O_{40}]\cdot 16H_2O$ 13

Fig. S4. Zoomed ^1H NMR spectrum of $Na_5[\{(C_6H_6)Ru\}_5VNb_{12}O_{40}]\cdot 16H_2O$ in D_2O. 13

Coupled HPLC-ESI-MS data 14

Fig. S5. Full scan mass spectra detected by a reversed-phase ion-pair high-performed liquid chromatography/electrospray ionization mass-spectrometry (RP-IP-HPLC/ESI-MS) for background (eluent) and resolved peaks 14

Fig. S6. Full scan mass spectra (RP-IP-HPLC/ESI-MS) for peak №1 (calculated patterns have negative intensities; ignored peaks refer to adduct ions of the eluents) 15

Table S4. The MS peaks assignment for HPLC peak №1 (Fig. S2-S5) 15

Fig. S7. Zoomed 3- and 2- area in RP-IP-HPLC/ESI-MS spectrum for HPLC peak №1 16

Fig. S8. Zoomed 940-980 m/z area in RP-IP-HPLC/ESI-MS spectrum for HPLC peak №1 16

Fig. S9. Zoomed 1420-1590 m/z area in RP-IP-HPLC/ESI-MS spectrum for HPLC peak №1. 17

Fig. S10. Full scan mass spectra (RP-IP-HPLC/ESI-MS) for HPLC peak №2 (calculated patterns have negative intensities; ignored peaks refer to adduct ions of the eluents) 17

Table S5. The MS peaks assignment for HPLC peak №2 (Figs. S6-S13) 18

Fig. S11. Zoomed 3- and 2- area in RP-IP-HPLC/ESI-MS spectrum for HPLC peak №2 18

Fig. S12. Zoomed 890-930 m/z area in RP-IP-HPLC/ESI-MS spectrum for HPLC peak №2 19

Fig. S13. Zoomed 970-1020 m/z area in RP-IP-HPLC/ESI-MS spectrum for HPLC peak №2 19

Fig. S14. Zoomed 1050-1090 m/z area in RP-IP-HPLC/ESI-MS spectrum for HPLC peak №2.....20
Fig. S15. Zoomed 1340-1400 m/z area in RP-IP-HPLC/ESI-MS spectrum for HPLC peak №2.....20
Fig. S16. Zoomed 1460-1520 m/z area in RP-IP-HPLC/ESI-MS spectrum for HPLC peak №2.....21
Fig. S17. Zoomed 1570-1720 m/z area in RP-IP-HPLC/ESI-MS spectrum for HPLC peak №2.....21
HR-ESI-MS data.....22
Fig. S18. HR-ESI-MS spectrum of $Na_5[\{(C_6H_6)Ru\}_5VNb_{12}O_{40}]\cdot 16H_2O$ crystals 22
Table S6. HR-ESI-MS peak assignments of $Na_5[\{(C_6H_6)Ru\}_5VNb_{12}O_{40}]\cdot 16H_2O$ aqueous solution 25

General information

All reagents were of commercial quality and were used as purchased. Elemental analysis was carried out on a Eurovector EA 3000 CHN analyser. Energy-dispersive X-ray spectroscopy (EDS) was performed on a Hitachi TM3000 TableTop SEM with Bruker QUANTAX 70 EDS equipment.

NMR

^{1}H NMR spectra were recorded on a Bruker Avance III 500 spectrometer using D_2O as internal standard. The ^{1}H NMR DOSY spectrum was recorded on a Bruker Avance 400 spectrometer at 400 MHz in a standard 5 mm tube. The spectrum was processed with NMR*Note*Book Software. ^{51}V NMR spectra were recorded on a Bruker Avance III 500 spectrometer. The CS were calibrated using Na_3VO_4 solution.

HR-ESI-MS

The high-resolution electrospray ionization mass spectrometric (HR-ESI-MS) measurements were performed at the Center of Collective Use «Mass spectrometric investigations» SB RAS. Spectra were obtained with a direct injection of liquid samples on an ESI quadrupole time-of-flight (ESI-q-TOF) high-resolution mass spectrometer Maxis 4G (Bruker Daltonics, Germany). The spectra were recorded in the 300-3000 m/z range in negative mode.

HPLC-ICP-AES

Separation was performed with HPLC system Milichrom A-02 (EcoNova, Russia) equipped with a two-beam spectrophotometric detector at the wavelength range of 190−360 nm in ion-pair mode of reversed phase chromatography (ProntoSIL 120-5-C18AQ, 2x75 mm), eluents: A – 0.01% tetrabutylammonium hydroxide, B – acetonitrile. Gradient elution with gradual increase in acetonitrile concentration was employed to resolve all the species. The gradient mode conditions: 0–2.4 min, 0–30% B; 2.4–4.8 min, 30% B; 4.8–9.3 min, 30-45% B; 9.3–10.6 min, 45-55% B; 10.6–14 min, 55% B; flow rate – 0.25 mL min^{-1}. Detection wavelength: 230 nm. ICP-AES spectrometer iCap 6500 Duo (Thermo Scientific, USA) with concentric nebulizer was applied as detector in hyphenated HPLC-ICP-AES. For the element detection Nb 202.9 nm, Ru 240.2 nm, V 292.4 nm spectral lines were selected. All measurements were performed in three replicates. The data acquisition and processing were carried out with iTEVA (Thermo Scientific, USA) software. The ICP-AES working parameters: power supply – 1150 W, nebulizer Ar flow rate – 0.70 L min^{-1}, auxiliary – 0.50 L min^{-1}, cooling – 12 L min^{-1}. In order to eliminate plasma quenching we diluted the liquid coming out of the column into the spray chamber with deionized water. The steady state of the plasma and the optimal values of analytical signals were finally achieved at the eluent flow rate of 0.25 mL min^{-1}, and the eluent velocity of 3 mL min^{-1} (peristaltic pump speed – 75 rpm).

HPLC-ESI-MS

Mass spectrometry analysis was carried out with quadrupole mass spectrometer Agilent 6130 MS. The electrospray ionization (ESI) was used as an ion source. The range of 300-3000 a.e.m. for negatively charged ions was monitored in SCAN mode of the HPLC-ESI-MS analysis. Nitrogen was used as the nebulizer gas (60 psi) and drying gas (7 L min^{-1}), the drying temperature was set at 350 °C; the capillary voltage was 4000 V and the optimal voltage for fragmentation of ions was 100 V. In SIM mode the monitoring of the mass of each component was realized throughout the

chromatographic run. A solution of the POM species in the mobile phase (eluents A and B) was continuously transferred from the HPLC column into the spray ionization camera of the mass spectrometer at a flow rate of 0.25 mL min^{-1}. After each experiment, mobile phase containing ion-pairing agents was thoroughly flushed out of the flow path to reduce contaminating the entire system over time. Experimental values of m/z in the spectrum were compared with calculated ones.

SCXRD

Crystallographic data and refinement details for **1** and **2** are given in Table S1. The diffraction data were collected on a New Xcalibur (Agilent Technologies) diffractometer with MoK_α radiation (λ = 0.71073) by doing φ scans of narrow (0.5°) frames at 140 K. Absorption correction was done empirically using SCALE3 ABSPACK (CrysAlisPro, Agilent Technologies, Version 1.171.37.35 (release 13-08-2014 CrysAlis171 .NET)). Structures were solved by SHELXT[1] and refined by full-matrix least-squares treatment against $|F|^2$ in anisotropic approximation with SHELX 2014/7[2] in ShelXle program.[3] Main geometrical parameters are present in Table S2. H-atoms of benzene ligands were refined in calculated positions, H-atoms of water molecules of crystallization were not refined. In both cases Na^+ and H_2O amounts have been found from the analytical techniques. After air-drying crystals of **1** and **2** lost a lot of water molecules of crystallization leading to amorphization of the solid samples. In the case of **2** SQUEEZE procedure[4] has been applied to remove highly disordered water molecules of crystallization and Na^+.

The crystallographic data have been deposed in the Cambridge Crystallographic Data Centre under the deposition codes CCDC 1504795 (**1**) and 2068338 (**2**).

References:

1 G. M. Sheldrick, *Acta Crystallogr. Sect. A Found. Adv.*, 2015, **71**, 3–8.

2 G. M. Sheldrick, *Acta Crystallogr. Sect. C Struct. Chem.*, 2015, **71**, 3–8.

3 C. B. Hübschle, G. M. Sheldrick and B. Dittrich, *J. Appl. Crystallogr.*, 2011, **44**, 1281–1284.

4 A. L. Spek, *Acta Crystallogr. Sect. C Struct. Chem.*, 2015, **71**, 9–18.

Table S1. Experimental details

	1	**2**
Chemical formula	$C_{24}H_{24}Na_{6.40}Nb_{12}O_{81.75}Ru_4V$	$C_{30}H_{30}Na_{4.55}Nb_{12}O_{64.25}Ru_5V$
M_r	3337.71	3194.35
Temperature (K)	130	140
a, b, c (Å)	19.0882 (3), 23.0497 (4), 25.0491 (6)	14.1141 (7), 16.3111 (10), 22.4722 (9)
α, β, γ (°)	114.402 (2), 100.742 (2), 101.388 (2)	92.167 (4), 93.075 (4), 114.998 (5)
V (Å^3)	9385.2 (4)	4671.6 (4)
Z	4	2
μ (mm^{-1})	2.27	2.40
Crystal size (mm)	0.18 × 0.08 × 0.06	0.18 × 0.10 × 0.08
T_{min}, T_{max}	0.926, 1.000	0.935, 1.000
No. of measured, independent and observed [$I > 2\sigma(I)$] reflections	76547, 35563, 23402	41461, 20631, 10168
R_{int}	0.053	0.086
θ values (°)	θ_{max} = 25.7, θ_{min} = 3.3	θ_{max} = 29.1, θ_{min} = 1.8
$(\sin\theta/\lambda)_{max}$ (Å^{-1})	0.610	0.684
Range of h, k, l	$-23 \le h \le 23$, $-28 \le k \le 23$, $-30 \le l \le 30$	$-18 \le h \le 19$, $-21 \le k \le 19$, $-30 \le l \le 29$
$R[F^2 > 2\sigma(F^2)]$, $wR(F^2)$, S	0.053, 0.113, 1.00	0.078, 0.193, 0.94
No. of reflections, parameters, restraints	35563, 2088, 24	20631, 1040, 204
Weighting scheme	$w = 1/[\sigma^2(F_o^2) + (0.0227P)^2]$ where $P = (F_o^2 + 2F_c^2)/3$	$w = 1/[\sigma^2(F_o^2) + (0.0735P)^2]$ where $P = (F_o^2 + 2F_c^2)/3$
$\Delta\rho_{max}$, $\Delta\rho_{min}$ (e Å^{-3})	1.74, -1.14	2.40, -1.19

Computer programs: *CrysAlis PRO* 1.171.38.41 (Rigaku OD, 2015), *SHELXS2014* (Sheldrick, 2014), *SHELXL2014* (Sheldrick, 2014), ShelXle (Hübschle, 2011), CIFTAB-2014 (Sheldrick, 2014).

Table S2. Selected geometric parameters (Å)

1			
O5—Ru4	2.117 (5)	O35—Nb19	2.070 (5)
O6—Ru4	2.089 (6)	O35—Nb24	2.057 (6)
O24—Ru4	2.099 (6)	O36—Nb7	2.063 (6)
O25—Ru2	2.145 (6)	O36—Nb19	2.044 (6)
O26—Ru2	2.123 (6)	O37—Nb3	1.984 (6)
O27—Ru3	2.095 (6)	O37—Nb15	2.099 (6)
O28—Ru2	2.080 (6)	O38—Nb3	1.907 (6)
O31—Ru1	2.144 (5)	O38—Nb17	1.923 (6)
O32—Ru1	2.108 (6)	O39—Nb1	2.063 (5)
O33—Ru1	2.133 (6)	O39—Nb3	2.052 (6)
O35—Ru3	2.109 (6)	O40—Nb1	2.056 (6)
O36—Ru3	2.113 (6)	O40—Nb23	2.045 (6)
O37—Ru5	2.140 (6)	O41—Nb3	2.058 (6)
O39—Ru8	2.105 (5)	O41—Nb23	2.082 (5)
O40—Ru8	2.118 (5)	O42—Nb15	1.920 (6)
O41—Ru8	2.101 (6)	O42—Nb23	1.920 (6)
O43—Ru5	2.092 (6)	O43—Nb15	2.033 (6)
O44—Ru5	2.137 (5)	O43—Nb21	2.037 (6)
O47—Ru7	2.094 (5)	O44—Nb17	1.999 (6)
O48—Ru7	2.082 (6)	O44—Nb21	2.080 (6)
O49—Ru7	2.144 (6)	O45—Nb10	2.442 (6)
O50—Ru6	2.115 (5)	O45—Nb17	2.433 (5)
O51—Ru6	2.100 (6)	O45—Nb22	2.407 (5)
O66—Ru6	2.104 (7)	O46—Nb1	1.932 (6)
O4—V1	1.707 (5)	O46—Nb10	1.918 (6)
O10—V2	1.709 (6)	O47—Nb2	2.067 (6)
O14—V2	1.715 (5)	O47—Nb4	2.065 (5)
O23—V1	1.708 (6)	O48—Nb2	2.044 (5)
O30—V1	1.711 (5)	O48—Nb18	2.072 (5)
O34—V1	1.703 (6)	O49—Nb4	2.066 (6)
O45—V2	1.724 (6)	O49—Nb18	2.068 (6)
O69—V2	1.708 (6)	O50—Nb10	2.081 (6)
O2—Nb8	1.925 (5)	O50—Nb22	2.055 (6)
O2—Nb16	1.942 (5)	O51—Nb10	2.059 (6)
O3—Nb4	1.937 (6)	O51—Nb17	2.066 (6)
O3—Nb10	1.944 (5)	O57—Nb16	1.753 (7)
O4—Nb5	2.407 (6)	O58—Nb24	1.738 (6)
O4—Nb9	2.426 (5)	O59—Nb8	1.766 (6)
O4—Nb16	2.425 (6)	O60—Nb3	1.767 (5)

O5—Nb8	2.057 (6)	O61—Nb10	1.756 (7)
O5—Nb13	2.054 (7)	O62—Nb6	1.763 (5)
O6—Nb6	2.026 (6)	O63—Nb9	1.766 (5)
O6—Nb8	2.094 (5)	O64—Nb5	1.773 (6)
O7—Nb5	1.942 (6)	O65—Nb4	1.773 (6)
O7—Nb19	1.904 (6)	O66—Nb17	2.036 (6)
O8—Nb18	1.915 (6)	O66—Nb22	2.105 (5)
O8—Nb20	1.971 (6)	O67—Nb1	1.921 (5)
O9—Nb5	1.934 (5)	O67—Nb4	1.931 (5)
O9—Nb13	1.927 (5)	O68—Nb11	2.017 (5)
O10—Nb15	2.438 (5)	O68—Nb14	1.928 (5)
O10—Nb20	2.431 (6)	O69—Nb1	2.441 (6)
O10—Nb21	2.450 (6)	O69—Nb3	2.404 (5)
O11—Nb11	1.985 (6)	O69—Nb23	2.420 (5)
O11—Nb16	1.938 (6)	O70—Nb7	1.946 (6)
O12—Nb2	1.928 (6)	O70—Nb12	1.935 (6)
O12—Nb23	1.912 (5)	O71—Nb13	1.914 (6)
O13—Nb7	1.919 (6)	O71—Nb19	1.937 (6)
O13—Nb9	1.925 (6)	O72—Nb8	1.939 (6)
O14—Nb2	2.445 (6)	O72—Nb14	1.934 (6)
O14—Nb4	2.423 (6)	O73—Nb21	1.928 (6)
O14—Nb18	2.404 (6)	O73—Nb22	1.913 (6)
O23—Nb11	2.407 (5)	O74—Nb13	1.780 (6)
O23—Nb12	2.465 (6)	O75—Nb20	2.009 (6)
O23—Nb14	2.451 (6)	O75—Nb21	1.923 (6)
O24—Nb6	2.052 (6)	O76—Nb2	1.908 (6)
O24—Nb13	2.076 (5)	O76—Nb20	1.989 (6)
O25—Nb6	1.984 (6)	O77—Nb6	1.902 (7)
O25—Nb14	2.086 (6)	O77—Nb24	1.937 (6)
O26—Nb12	2.090 (5)	O78—Nb11	2.015 (6)
O26—Nb24	1.988 (6)	O78—Nb12	1.924 (6)
O27—Nb7	2.074 (5)	O79—Nb1	1.756 (6)
O27—Nb24	2.063 (6)	O80—Nb15	1.901 (6)
O28—Nb12	2.042 (6)	O80—Nb20	2.019 (5)
O28—Nb14	2.021 (6)	O81—Nb18	1.971 (6)
O29—Nb9	1.916 (6)	O81—Nb22	1.926 (5)
O29—Nb11	1.983 (6)	O82—Nb2	1.781 (5)
O30—Nb6	2.441 (5)	O83—Nb23	1.767 (6)
O30—Nb8	2.420 (6)	O84—Nb19	1.777 (6)
O30—Nb13	2.412 (6)	O85—Nb14	1.762 (6)
O31—Nb5	2.036 (6)	O87—Nb12	1.761 (6)

O31—Nb16	2.076 (6)	O88—Nb11	1.755 (6)
O32—Nb9	2.040 (6)	O89—Nb7	1.761 (6)
O32—Nb16	2.068 (5)	O90—Nb22	1.767 (6)
O33—Nb5	2.042 (5)	O92—Nb20	1.754 (6)
O33—Nb9	2.074 (6)	O93—Nb17	1.765 (6)
O34—Nb7	2.438 (5)	O99—Nb15	1.782 (6)
O34—Nb19	2.441 (6)	O100—Nb18	1.755 (6)
O34—Nb24	2.432 (5)	O112—Nb21	1.767 (7)
2			
O2—Ru1	2.133 (9)	O18—Nb5	2.050 (9)
O3—Ru1	2.086 (8)	O18—Nb8	2.046 (9)
O4—Ru1	2.143 (8)	O19—Nb4	2.041 (8)
O6—Ru5	2.098 (9)	O19—Nb5	2.079 (8)
O10—Ru2	2.100 (8)	O20—Nb5	1.768 (9)
O11—Ru2	2.127 (10)	O21—Nb4	2.432 (8)
O12—Ru2	2.114 (9)	O21—Nb5	2.408 (8)
O16—Ru4	2.102 (9)	O21—Nb8	2.416 (9)
O18—Ru4	2.149 (9)	O22—Nb3	2.436 (8)
O19—Ru4	2.087 (9)	O22—Nb9	2.462 (8)
O24—Ru5	2.156 (9)	O22—Nb10	2.426 (9)
O36—Ru5	2.164 (9)	O24—Nb2	1.993 (8)
O38—Ru3	2.120 (8)	O24—Nb10	2.007 (8)
O39—Ru3	2.096 (8)	O25—Nb10	1.924 (8)
O40—Ru3	2.114 (9)	O25—Nb12	1.924 (8)
O21—V1	1.714 (10)	O26—Nb9	1.900 (9)
O22—V1	1.694 (8)	O26—Nb11	1.949 (9)
O32—V1	1.695 (8)	O27—Nb11	1.754 (9)
O35—V1	1.717 (8)	O28—Nb8	1.909 (9)
O1—Nb1	1.733 (9)	O28—Nb11	1.930 (9)
O2—Nb1	2.046 (8)	O29—Nb5	1.917 (8)
O2—Nb4	1.997 (9)	O29—Nb6	1.917 (9)
O3—Nb1	2.083 (9)	O30—Nb1	1.950 (9)
O3—Nb2	1.996 (8)	O30—Nb7	1.956 (8)
O4—Nb2	1.999 (9)	O31—Nb1	1.922 (9)
O4—Nb3	2.025 (8)	O31—Nb5	1.958 (9)
O5—Nb2	1.738 (9)	O32—Nb1	2.439 (8)
O6—Nb2	1.991 (9)	O32—Nb2	2.486 (9)
O6—Nb7	2.048 (9)	O32—Nb7	2.439 (8)
O7—Nb4	1.739 (10)	O33—Nb7	1.744 (9)
O8—Nb3	1.919 (10)	O34—Nb6	1.943 (9)

O8—Nb4	1.924 (9)	O34—Nb7	1.942 (9)
O9—Nb3	1.747 (9)	O35—Nb6	2.426 (8)
O10—Nb3	2.037 (9)	O35—Nb11	2.435 (8)
O10—Nb10	2.051 (8)	O35—Nb12	2.402 (9)
O11—Nb3	2.001 (9)	O36—Nb7	2.045 (8)
O11—Nb9	2.080 (9)	O36—Nb12	1.992 (8)
O12—Nb9	2.080 (10)	O37—Nb12	1.741 (10)
O12—Nb10	2.009 (9)	O38—Nb11	2.065 (9)
O13—Nb10	1.742 (10)	O38—Nb12	2.050 (8)
O14—Nb9	1.743 (9)	O39—Nb6	2.036 (9)
O15—Nb8	1.915 (9)	O39—Nb12	2.047 (8)
O15—Nb9	1.925 (10)	O40—Nb6	2.027 (8)
O16—Nb4	2.045 (9)	O40—Nb11	2.060 (8)
O16—Nb8	2.065 (9)	O41—Nb6	1.745 (8)
O17—Nb8	1.782 (10)		

Synthesis

Synthesis of $Na_9H_4[VNb_{12}O_{40}\{NbO(CO_3)\}_2]\cdot 34H_2O$ (reported in our previous paper 10.1021/acs.inorgchem.6b02108):

$Na_7H[Nb_6O_{19}]\cdot 15H_2O$ (0.400 g, 0.31 mmol) was dissolved in 10 mL H_2O upon heating. Then $NaVO_3\cdot 2H_2O$ (0.046 g, 0.31 mmol) and $NaHCO_3$ (0.150 g, 1.79 mmol) were added quickly one after the other. The clear solution was placed into an autoclave and was kept at 220 °C for 18h. After colling a colorless precipitate was centrifuged, the filtrate was reduced in volume by heating at 90°C to 3 mL. The concentrated solution was placed into a vial for slow evaporation. After 2 days colorless crystals were formed.

^{51}V NMR (H_2O+D_2O, r.t.): -461.02, -466.88, - 472.39, -474.54, -480.11, -512.48 ppm. (Fig. S1)

Synthesis of $Na_6H[\alpha\text{-}\{(C_6H_6)Ru\}_4VNb_{12}O_{40}]\cdot 41.25H_2O$ (1) and $Na_5[\{(C_6H_6)Ru\}_5VNb_{12}O_{40}]\cdot 16H_2O$ (2):

0.440 g (0.15 mmol) of $Na_9H_4[VNb_{12}O_{40}\{NbO(CO_3)\}_2]\cdot 34H_2O$ was dissolved in 25 mL H_2O upon heating, then 0.150 g (0.30 mmol) of $[(C_6H_6)RuCl_2]_2$ was added to the clear solution. Reaction mixture was heated for 48 h at 90°C. To final brown solution a large excess of acetone was added for precipitation (solid A). While slow diffusion typically gives brown solid and small amount of complex **1** crystals (EDX (Hitachi TM 3000) calc. Na; Ru; Nb; V: 8.0; 23.7; 65.3; 3.0; found Na; Ru; Nb; V: 8.4; 23.2; 65.8; 3.6. Analysis found C, H (%) 8.1, 2.9; calcl. C, H (%) 8.5, 3.2).

The solid A was centrifuged and washed with acetone. Dry solid material was dissolved in methanol. Non-soluble residue does not contain vanadium in the composition (according to ^{51}V NMR), so it was removed from solution. The filtrate was chromatographed on silica gel (eluent – methanol). The brown fraction was collected and evaporated on air to dryness, then solid material was dissolved in minimal amount of water. Orange crystals of $Na_5[\{(C_6H_6)Ru\}_5VNb_{12}O_{40}]\cdot 16H_2O$ was obtained by layering technique with i-PrOH. Together with the crystals, an amorphous material is formed. They can be separated by filtration on glass filter with large pores. An additional portion of crystals can be obtained by recrystallizing the amorphous material by layering i-PrOH. Yield: 0.150 g (34%) based on Ru.

^{51}V NMR (Fig. S2) (H_2O+D_2O): singlet at -467.33 ppm.

IR (Fig. S3) (ATR, cm^{-1}): 1631 (m), 1434 (m), 1350 (w), 1332 (w), 1150 (w), 1088 (w), 1008 (w), 980 (w), 927 (m), 866 (s), 785 (vs), 653 (vs), 633 (vs), 617 (vs), 606 (vs), 590 (vs), 577 (vs), 568 (vs), 554 (vs).

^1H NMR (H_2O+D_2O): **6.18**, 6.14, 6.12, 6.10, **5.92**, 5.90, 5.88, 5.85, 5.83, 5.81, **5.78**, 5.77. The most intense signals with 2:1:2 ratio (highlighted in bold) are from current symmetrical isomer.

ICP-AES found Na, V, Nb, Ru (%): 3.3, 1.7, 35.7, 16.2; calcd for $Na_5[\{(C_6H_6)Ru\}_5VNb_{12}O_{40}]\cdot 16H_2O$ Na, V, Nb, Ru (%): 3.7, 1.6, 35.9, 16.3.

CHN analysis: found C, H (%): 11.6, 1.8; calcd for $Na_5[\{(C_6H_6)Ru\}_5VNb_{12}O_{40}]\cdot 16H_2O$ C, H (%): 11.6, 2.0.

Table S3. Atomic ratios Nb/V and Nb/Ru calculated from HPLC-ICP-AES-data

Peak	Anion	Nb/V	Nb/Ru
1	$[\{Ru(C_6H_6)\}_4VNb_{12}O_{40}]^{7-}$	12.0±0.5	3.0±0.3
2	$[\{Ru(C_6H_6)\}_3VNb_{12}O_{40}]^{9-}$	12.0±0.5	4.0±0.3

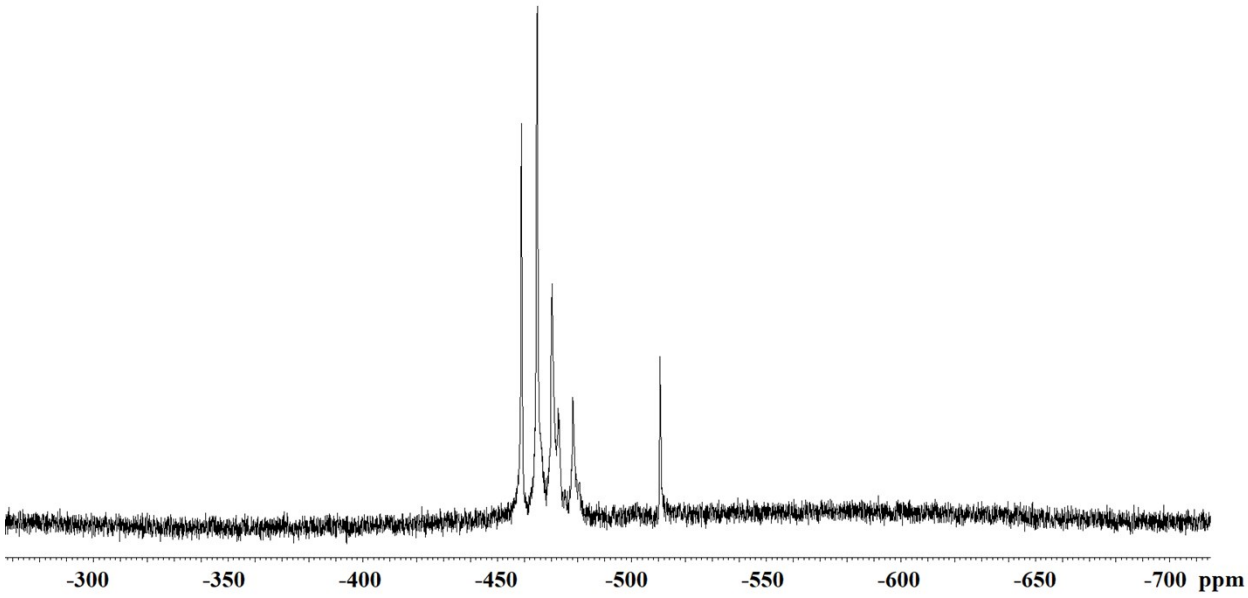

Fig. S1. ^{51}V NMR spectrum of $Na_9H_4[VNb_{12}O_{40}\{NbO(CO_3)\}_2]\cdot 34H_2O$ in D_2O

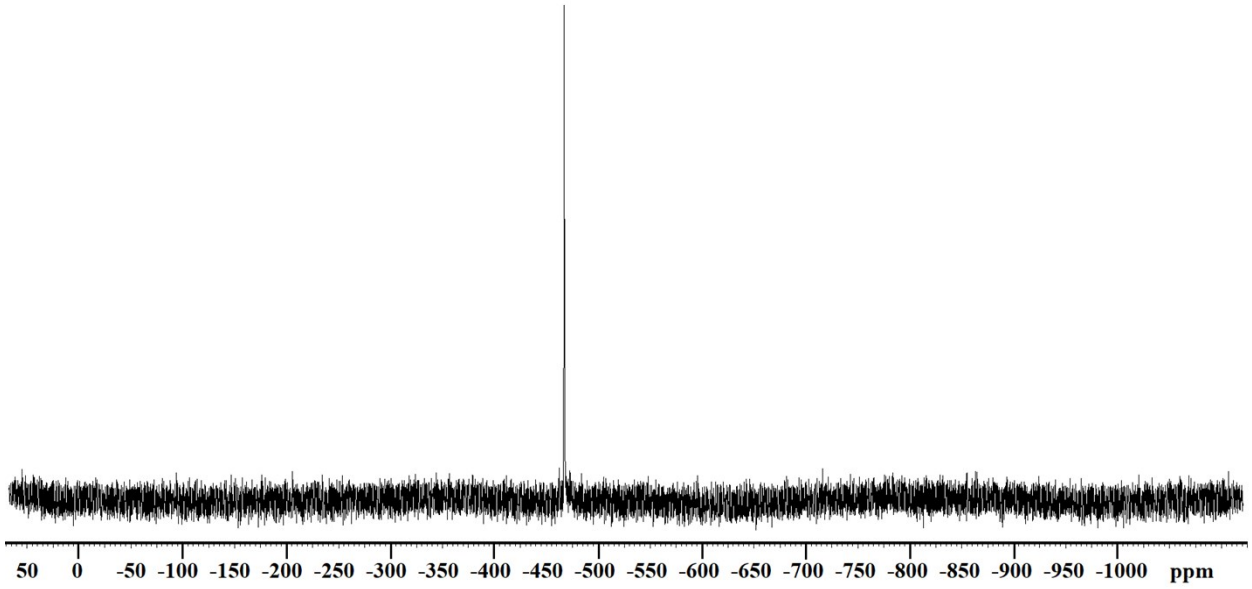

Fig. S2. ^{51}V NMR spectrum of $Na_5[\{(C_6H_6)Ru\}_5VNb_{12}O_{40}]\cdot 16H_2O$ in D_2O

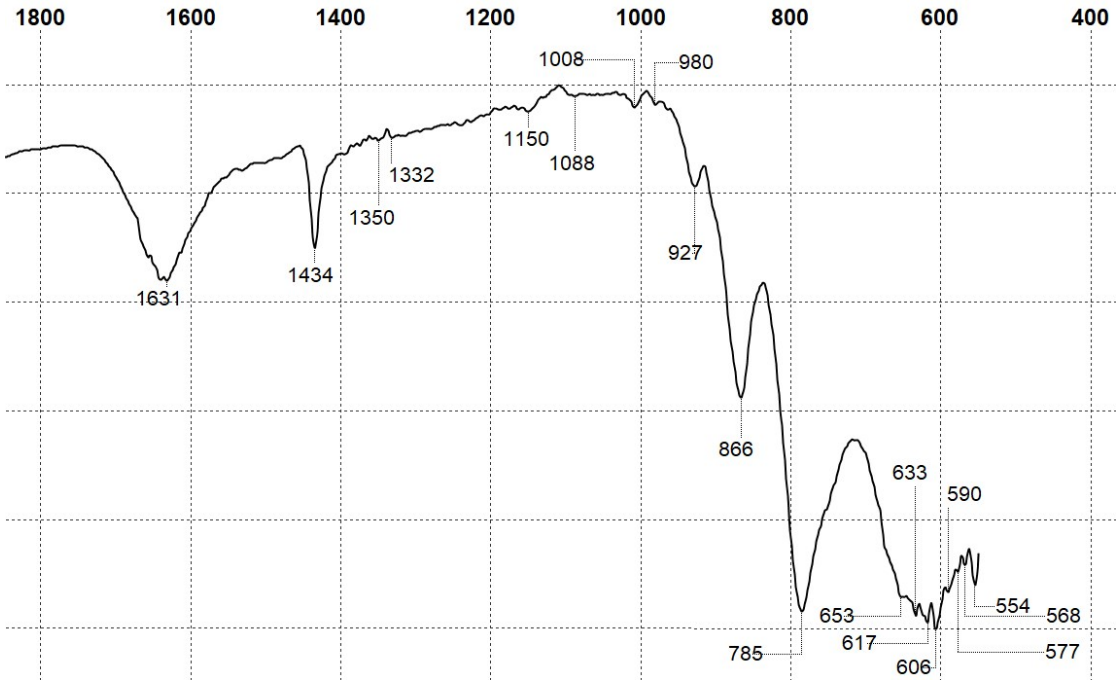

Fig. S3. IR spectrum of $Na_5[\{(C_6H_6)Ru\}_5VNb_{12}O_{40}]\cdot 16H_2O$

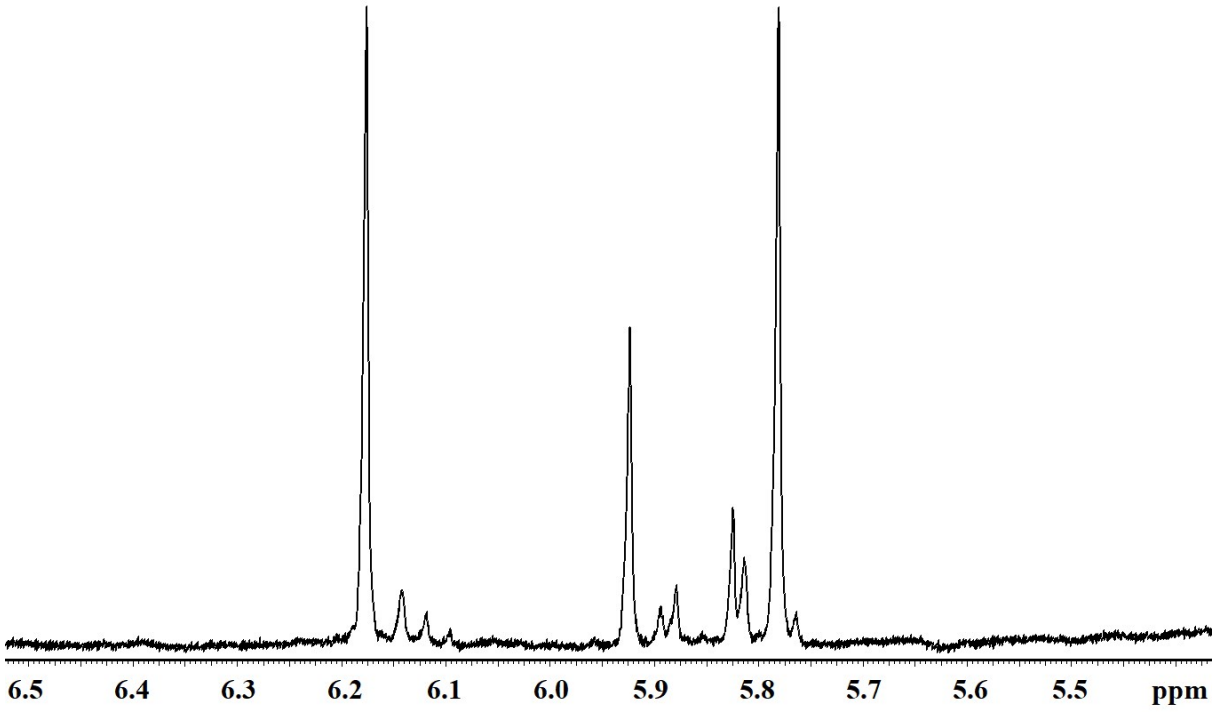

Fig. S4. Zoomed ^1H NMR spectrum of $Na_5[\{(C_6H_6)Ru\}_5VNb_{12}O_{40}]\cdot 16H_2O$ in D_2O.

Coupled HPLC-ESI-MS data

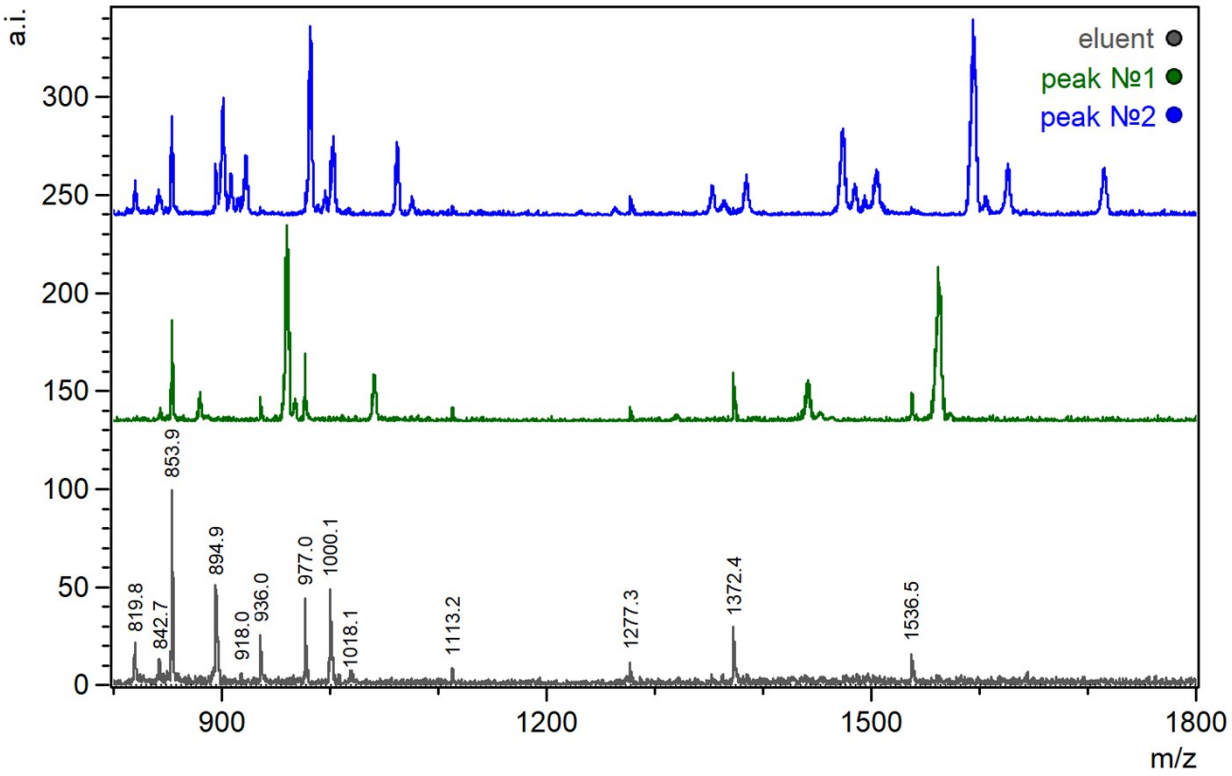

Fig. S5. Full scan mass spectra detected by a reversed-phase ion-pair high-performed liquid chromatography/electrospray ionization mass-spectrometry (RP-IP-HPLC/ESI-MS) for background (eluent) and resolved peaks

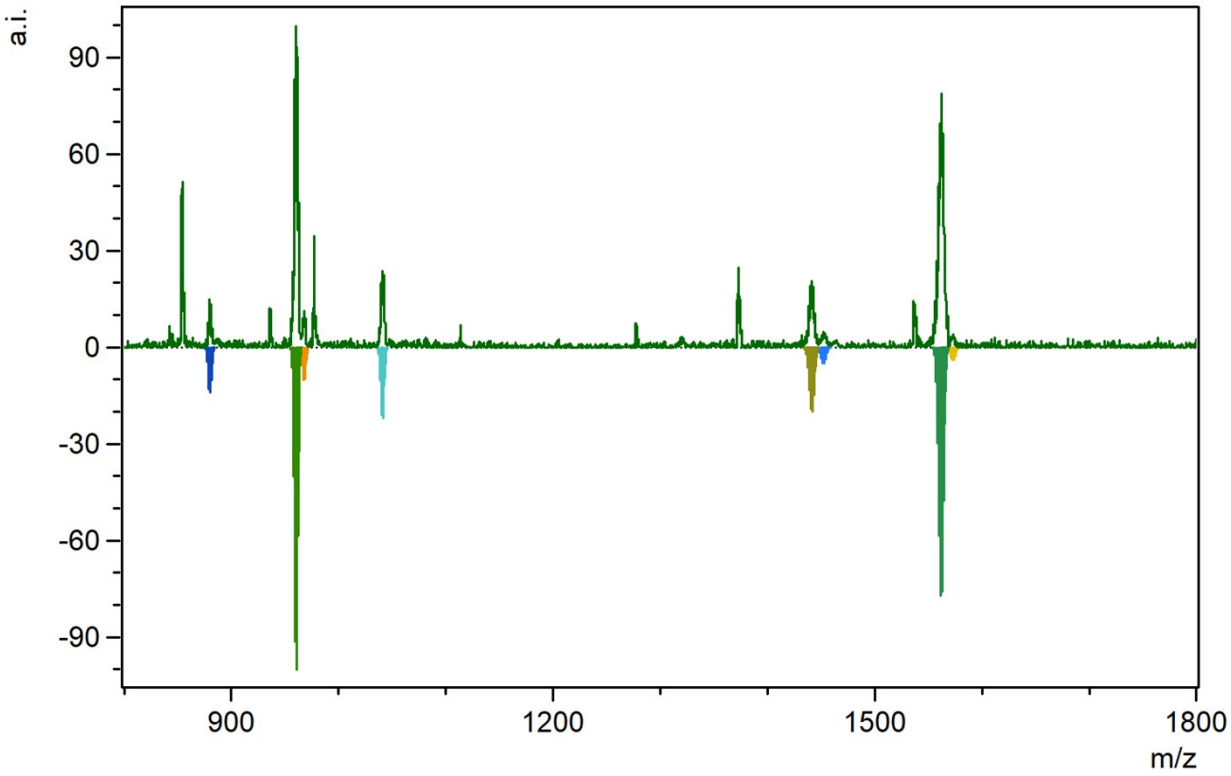

Fig. S6. Full scan mass spectra (RP-IP-HPLC/ESI-MS) for peak №1 (calculated patterns have negative intensities; ignored peaks refer to adduct ions of the eluents)

Table S4. The MS peaks assignment for HPLC peak №1 (Fig. S2-S5)

Ion composition	exp	calc
$[\{(C_6H_6)Ru\}_4VNb_{12}O_{40} + Na + 3H + CH_3OH + CH_3CN + H_2O]^{3-}$	879.8	879.9
$[\{(C_6H_6)Ru\}_4VNb_{12}O_{40} + Na + 2H + TBA + CH_3OH + CH_3CN + H_2O]^{3-}$	960.4	960.4
$[\{(C_6H_6)Ru\}_4VNb_{12}O_{40} + 2Na + H + TBA + CH_3OH + CH_3CN + H_2O]^{3-}$	967.8	967.7
$[\{(C_6H_6)Ru\}_4VNb_{12}O_{40} + Na + H + 2TBA + CH_3OH + CH_3CN + H_2O]^{3-}$	1040.8	1040.8
$[\{(C_6H_6)Ru\}_4VNb_{12}O_{40} + Na + 3H + TBA + CH_3OH + CH_3CN + H_2O]^{2-}$	1441.1	1441.0
$[\{(C_6H_6)Ru\}_4VNb_{12}O_{40} + 2Na + 2H + TBA + CH_3OH + CH_3CN + H_2O]^{2-}$	1451.9	1452.0
$[\{(C_6H_6)Ru\}_4VNb_{12}O_{40} + Na + 2H + 2TBA + CH_3OH + CH_3CN + H_2O]^{2-}$	1561.9	1561.8
$[\{(C_6H_6)Ru\}_4VNb_{12}O_{40} + 2Na + H + 2TBA + CH_3OH + CH_3CN + H_2O]^{2-}$	1572.8	1572.8

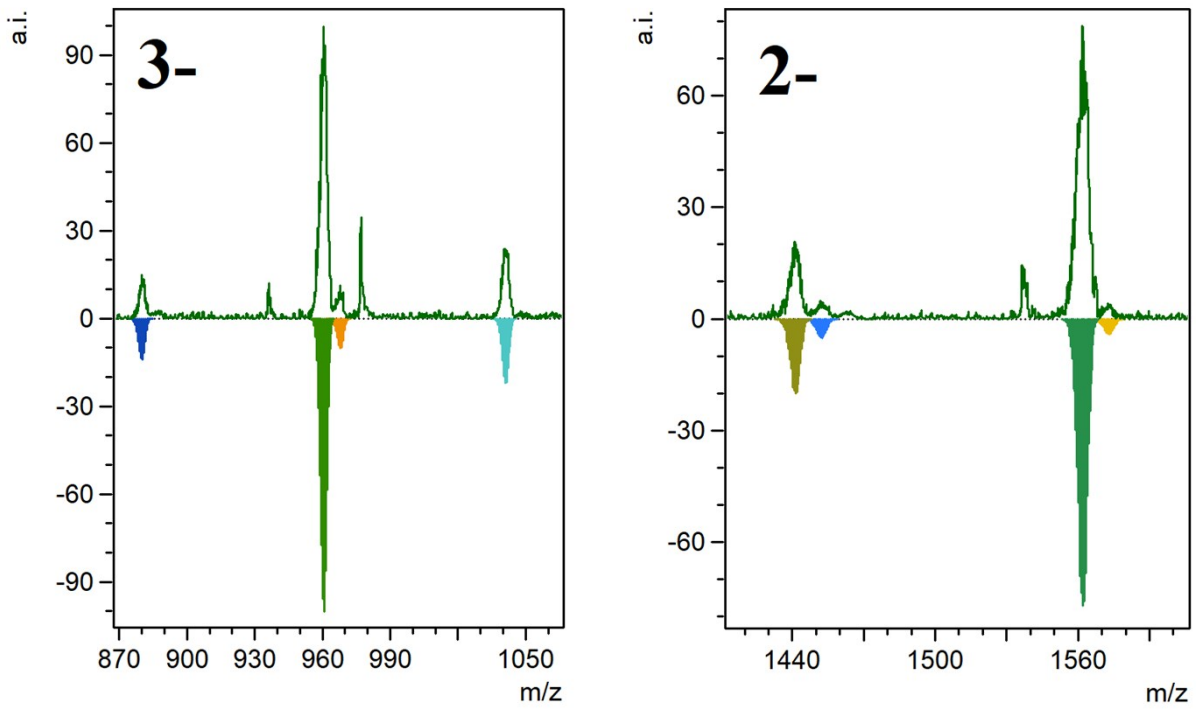

Fig. S7. Zoomed 3- and 2- area in RP-IP-HPLC/ESI-MS spectrum for HPLC peak №1

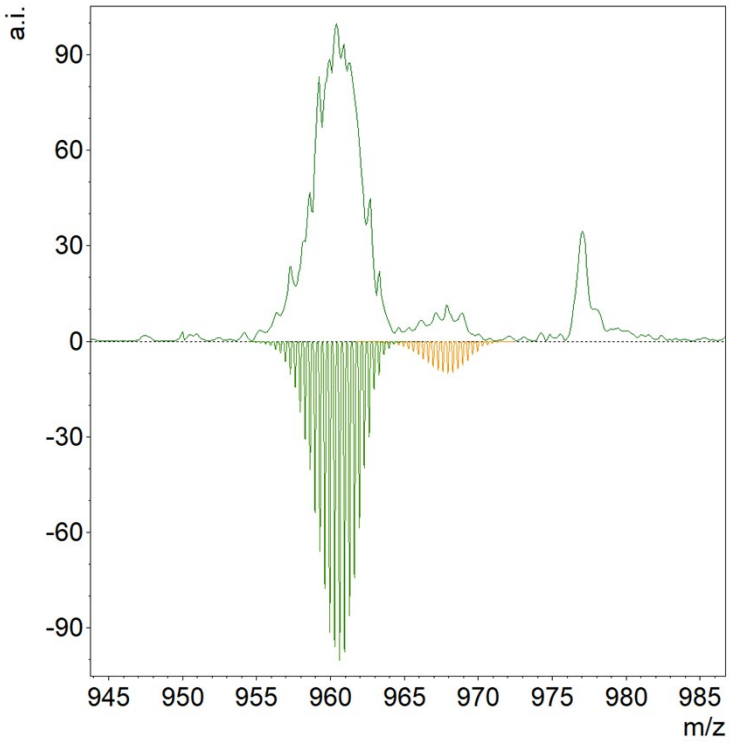

Fig. S8. Zoomed 940-980 m/z area in RP-IP-HPLC/ESI-MS spectrum for HPLC peak №1

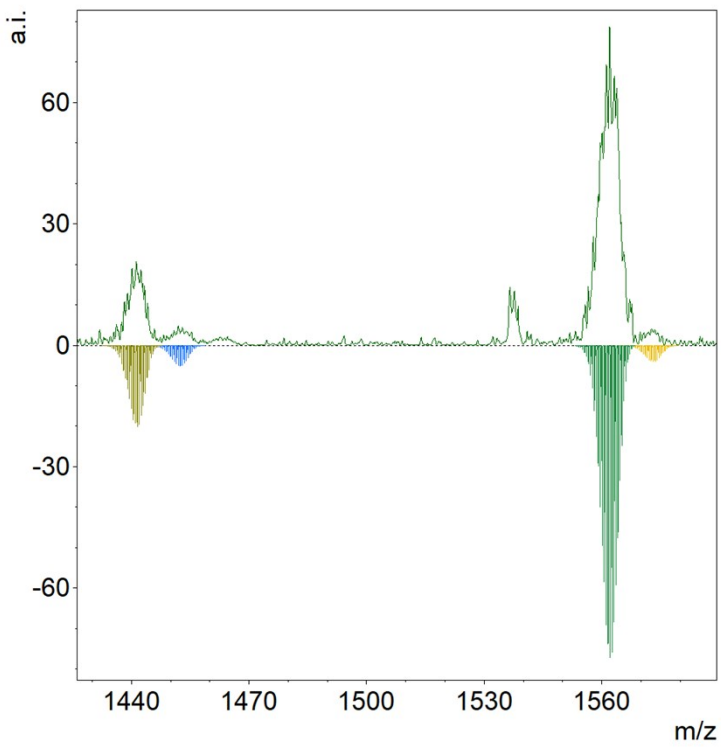

Fig. S9. Zoomed 1420-1590 m/z area in RP-IP-HPLC/ESI-MS spectrum for HPLC peak №1.

Fig. S10. Full scan mass spectra (RP-IP-HPLC/ESI-MS) for HPLC peak №2 (calculated patterns have negative intensities; ignored peaks refer to adduct ions of the eluents)

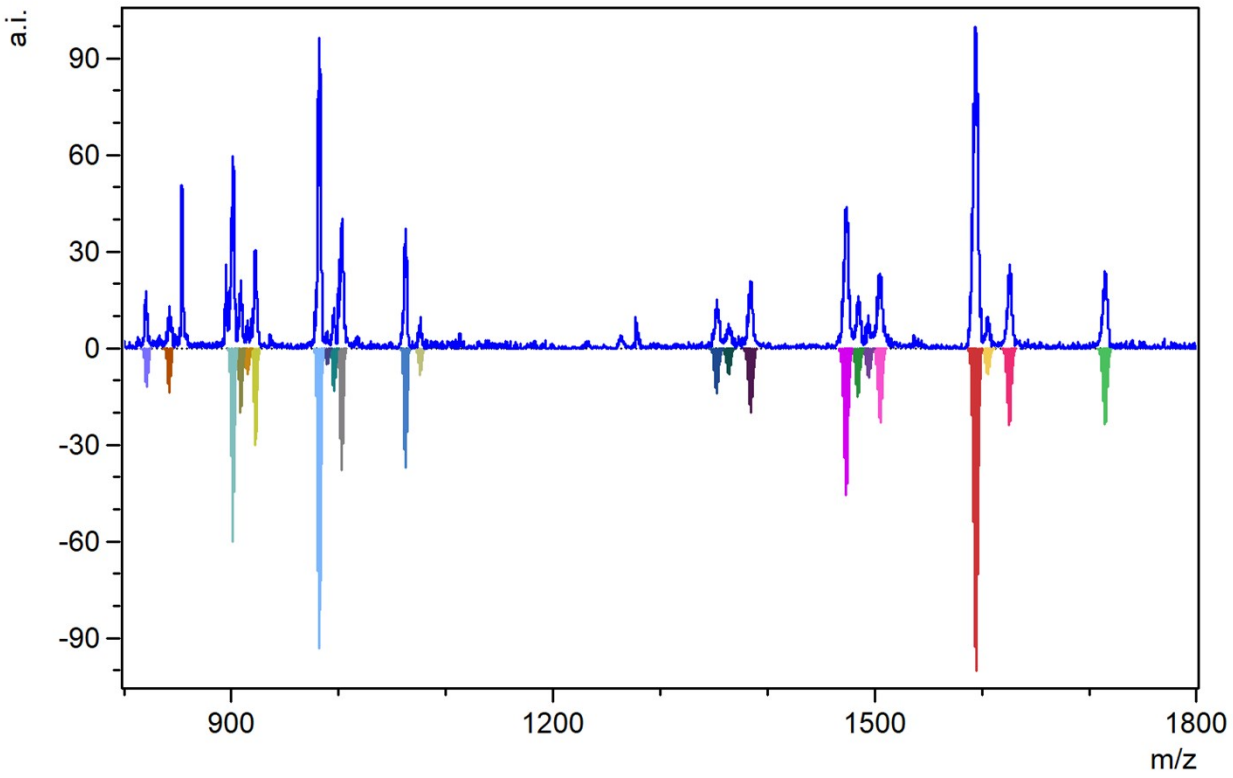

Table S5. The MS peaks assignment for HPLC peak №2 (Figs. S6-S13)

Ion composition	exp	calc
$[\{(C_6H_6)Ru\}_3VNb_{12}O_{40} + Na + 5H + CH_3OH + CH_3CN + H_2O]^{3-}$	820.9	820.8
$[\{(C_6H_6)Ru\}_3VNb_{12}O_{40} + 2Na + 4H + CH_3OH + 2CH_3CN + H_2O]^{3-}$	841.9	841.8
$[\{(C_6H_6)Ru\}_3VNb_{12}O_{40} + Na + 4H + TBA + CH_3OH + CH_3CN + H_2O]^{3-}$	901.3	901.3
$[\{(C_6H_6)Ru\}_3VNb_{12}O_{40} + 2Na + 3H + TBA + CH_3OH + CH_3CN + H_2O]^{3-}$	908.7	908.6
$[\{(C_6H_6)Ru\}_3VNb_{12}O_{40} + Na + 4H + TBA + CH_3OH + 2CH_3CN + H_2O]^{3-}$	915.0	914.9
$[\{(C_6H_6)Ru\}_3VNb_{12}O_{40} + 2Na + 3H + TBA + CH_3OH + 2CH_3CN + H_2O]^{3-}$	922.3	922.3
$[\{(C_6H_6)Ru\}_3VNb_{12}O_{40} + Na + 3H + 2TBA + CH_3OH + CH_3CN + H_2O]^{3-}$	981.8	981.8
$[\{(C_6H_6)Ru\}_3VNb_{12}O_{40} + 2Na + 2H + 2TBA + CH_3OH + CH_3CN + H_2O]^{3-}$	989.0	989.1
$[\{(C_6H_6)Ru\}_3VNb_{12}O_{40} + Na + 3H + 2TBA + CH_3OH + 2CH_3CN + H_2O]^{3-}$	995.6	995.5
$[\{(C_6H_6)Ru\}_3VNb_{12}O_{40} + 2Na + 2H + 2TBA + CH_3OH + 2CH_3CN + H_2O]^{3-}$	1002.8	1002.8
$[\{(C_6H_6)Ru\}_3VNb_{12}O_{40} + Na + 2H + 3TBA + CH_3OH + CH_3CN + H_2O]^{3-}$	1062.3	1062.3
$[\{(C_6H_6)Ru\}_3VNb_{12}O_{40} + Na + 2H + 3TBA + CH_3OH + 2CH_3CN + H_2O]^{3-}$	1076.1	1076.0
$[\{(C_6H_6)Ru\}_3VNb_{12}O_{40} + Na + 5H + TBA + CH_3OH + CH_3CN + H_2O]^{2-}$	1352.4	1352.5
$[\{(C_6H_6)Ru\}_3VNb_{12}O_{40} + 2Na + 4H + TBA + CH_3OH + CH_3CN + H_2O]^{2-}$	1363.5	1363.5
$[\{(C_6H_6)Ru\}_3VNb_{12}O_{40} + 2Na + 4H + TBA + CH_3OH + 2CH_3CN + H_2O]^{2-}$	1384.1	1384.0
$[\{(C_6H_6)Ru\}_3VNb_{12}O_{40} + Na + 4H + 2TBA + CH_3OH + CH_3CN + H_2O]^{2-}$	1473.2	1473.2
$[\{(C_6H_6)Ru\}_3VNb_{12}O_{40} + 2Na + 3H + 2TBA + CH_3OH + CH_3CN + H_2O]^{2-}$	1484.1	1484.2
$[\{(C_6H_6)Ru\}_3VNb_{12}O_{40} + Na + 4H + 2TBA + CH_3OH + 2CH_3CN + H_2O]^{2-}$	1493.7	1493.7
$[\{(C_6H_6)Ru\}_3VNb_{12}O_{40} + 2Na + 3H + 2TBA + CH_3OH + 2CH_3CN + H_2O]^{2-}$	1504.6	1504.7
$[\{(C_6H_6)Ru\}_3VNb_{12}O_{40} + Na + 3H + 3TBA + CH_3OH + CH_3CN + H_2O]^{2-}$	1594.0	1593.9
$[\{(C_6H_6)Ru\}_3VNb_{12}O_{40} + 2Na + 2H + 3TBA + CH_3OH + CH_3CN + H_2O]^{2-}$	1604.9	1604.9
$[\{(C_6H_6)Ru\}_3VNb_{12}O_{40} + 2Na + 2H + 3TBA + CH_3OH + 2CH_3CN + H_2O]^{2-}$	1625.4	1625.4
$[\{(C_6H_6)Ru\}_3VNb_{12}O_{40} + Na + 2H + 4TBA + CH_3OH + CH_3CN + H_2O]^{2-}$	1714.6	1714.6

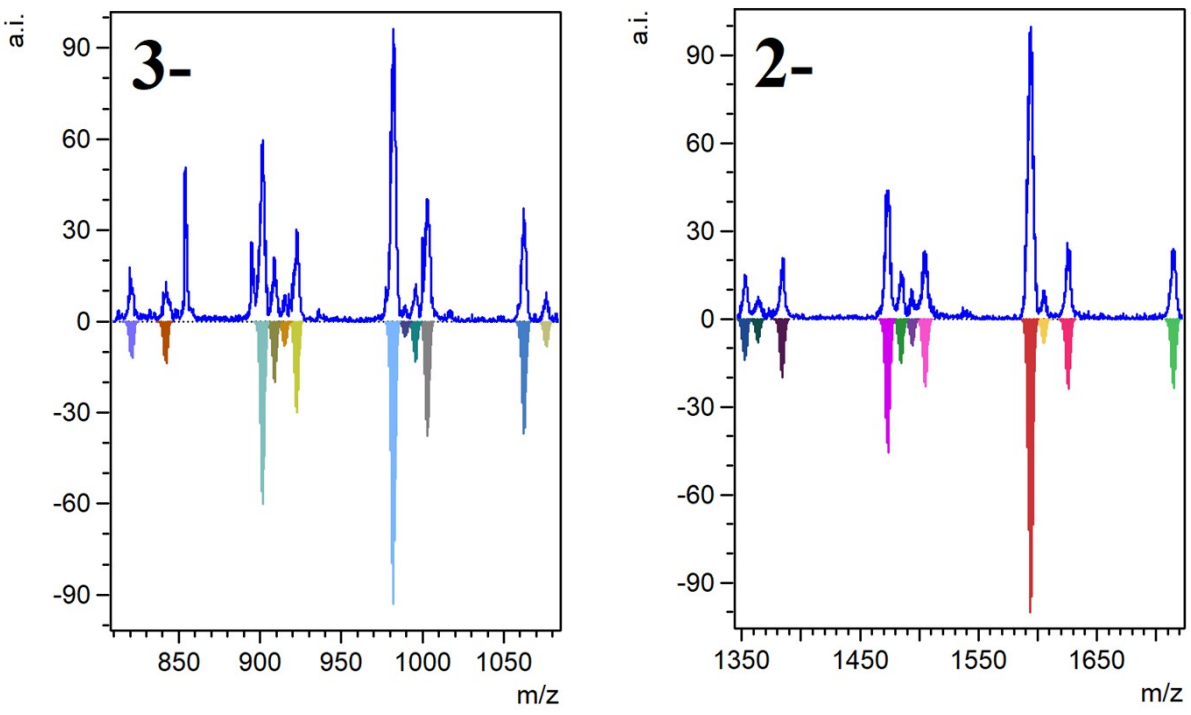

Fig. S11. Zoomed 3- and 2- area in RP-IP-HPLC/ESI-MS spectrum for HPLC peak №2

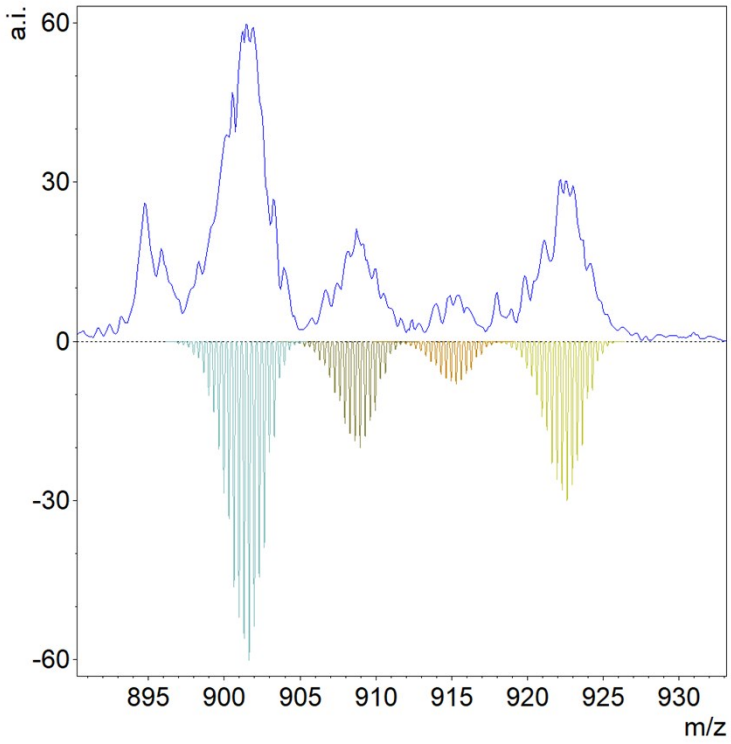

Fig. S12. Zoomed 890-930 m/z area in RP-IP-HPLC/ESI-MS spectrum for HPLC peak №2

Fig. S13. Zoomed 970-1020 m/z area in RP-IP-HPLC/ESI-MS spectrum for HPLC peak №2

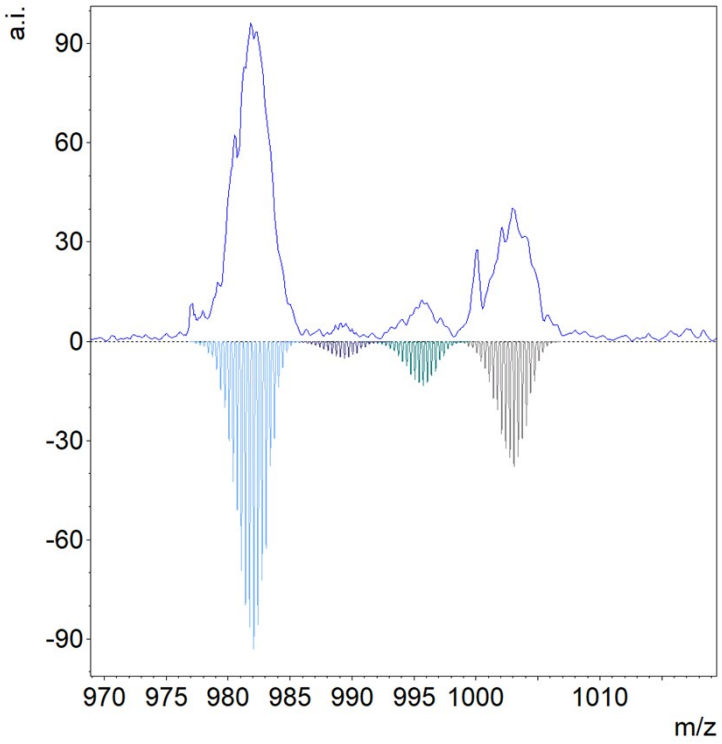

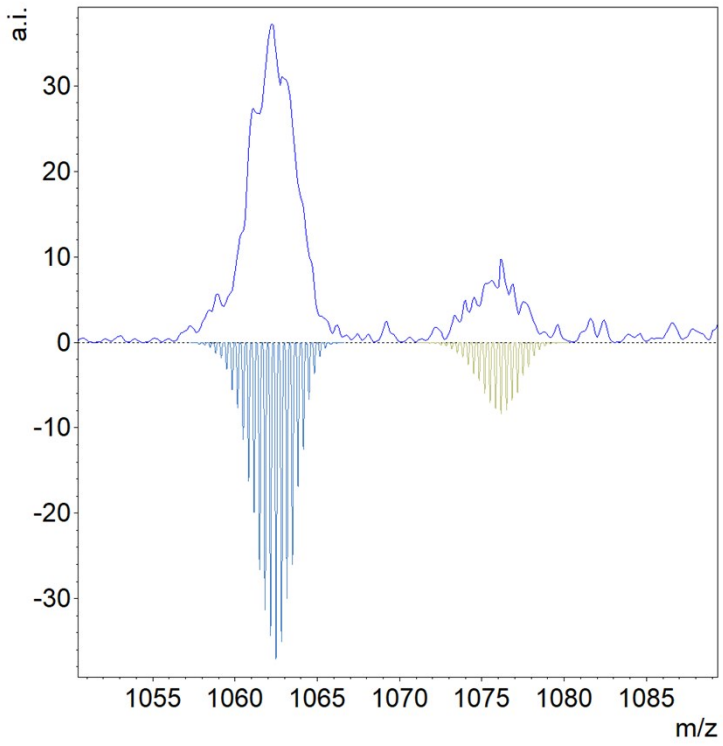

Fig. S14. Zoomed 1050-1090 m/z area in RP-IP-HPLC/ESI-MS spectrum for HPLC peak №2

Fig. S15. Zoomed 1340-1400 m/z area in RP-IP-HPLC/ESI-MS spectrum for HPLC peak №2

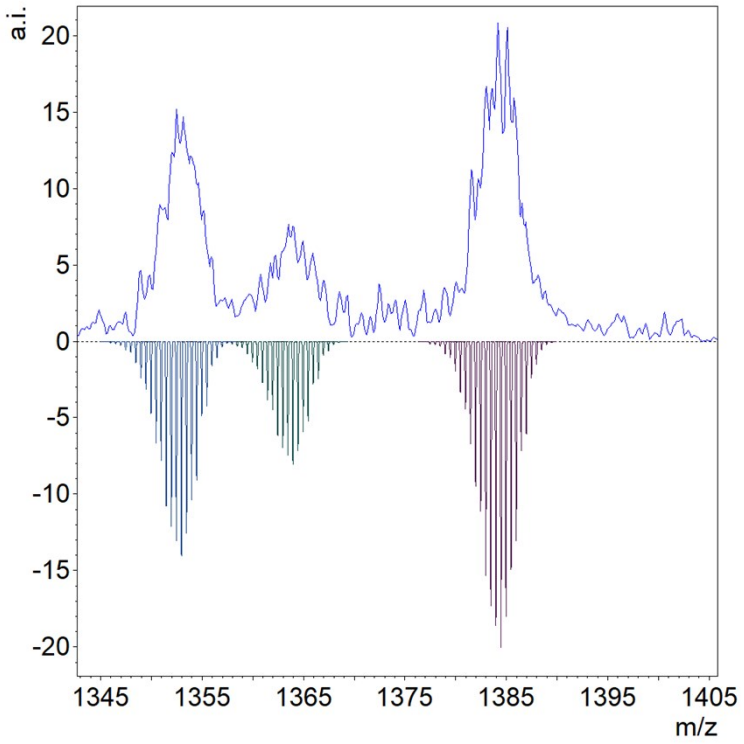

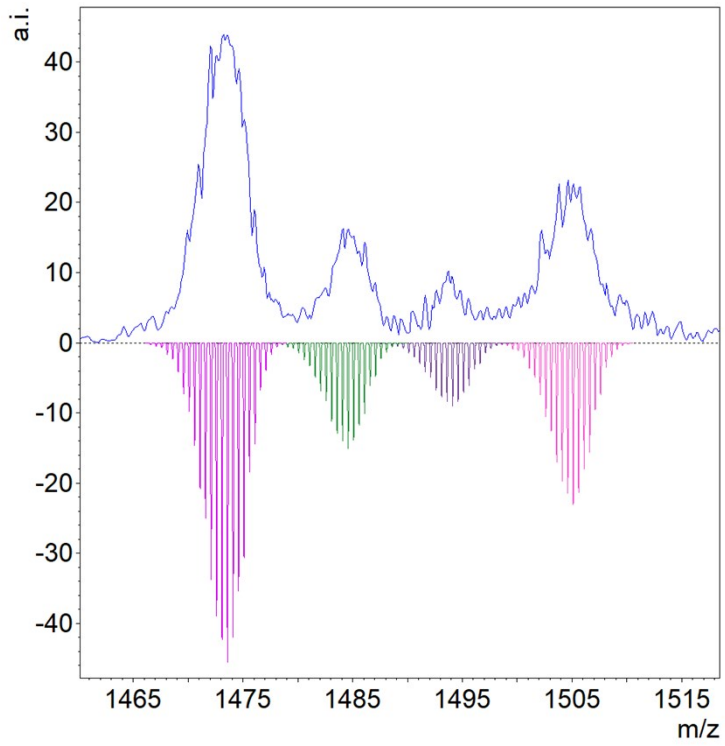

Fig. S16. Zoomed 1460-1520 m/z area in RP-IP-HPLC/ESI-MS spectrum for HPLC peak №2

Fig. S17. Zoomed 1570-1720 m/z area in RP-IP-HPLC/ESI-MS spectrum for HPLC peak №2

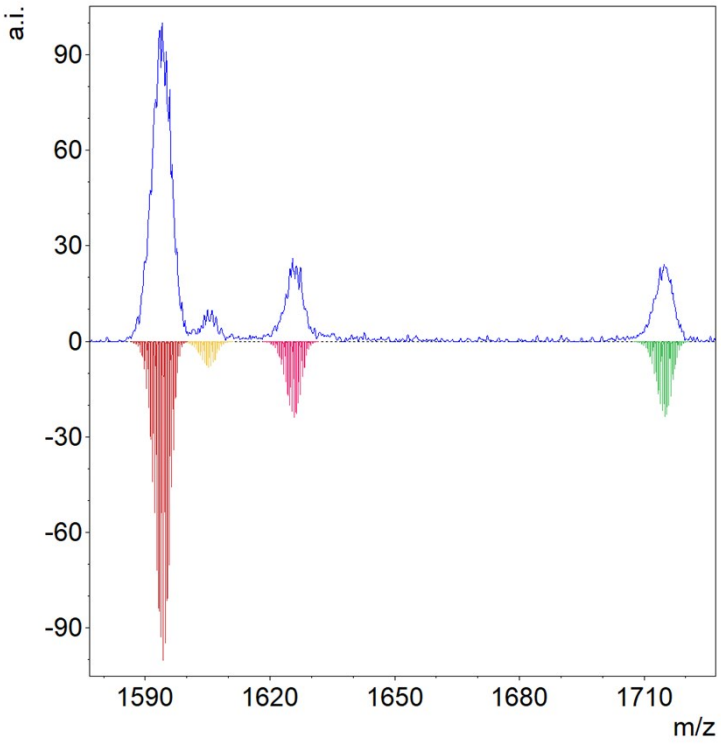

HR-ESI-MS data

Fig. S18. HR-ESI-MS spectrum of $Na_5[\{(C_6H_6)Ru\}_5VNb_{12}O_{40}]\cdot 16H_2O$ crystals

a) Full spectrum (600-3000 m/z)

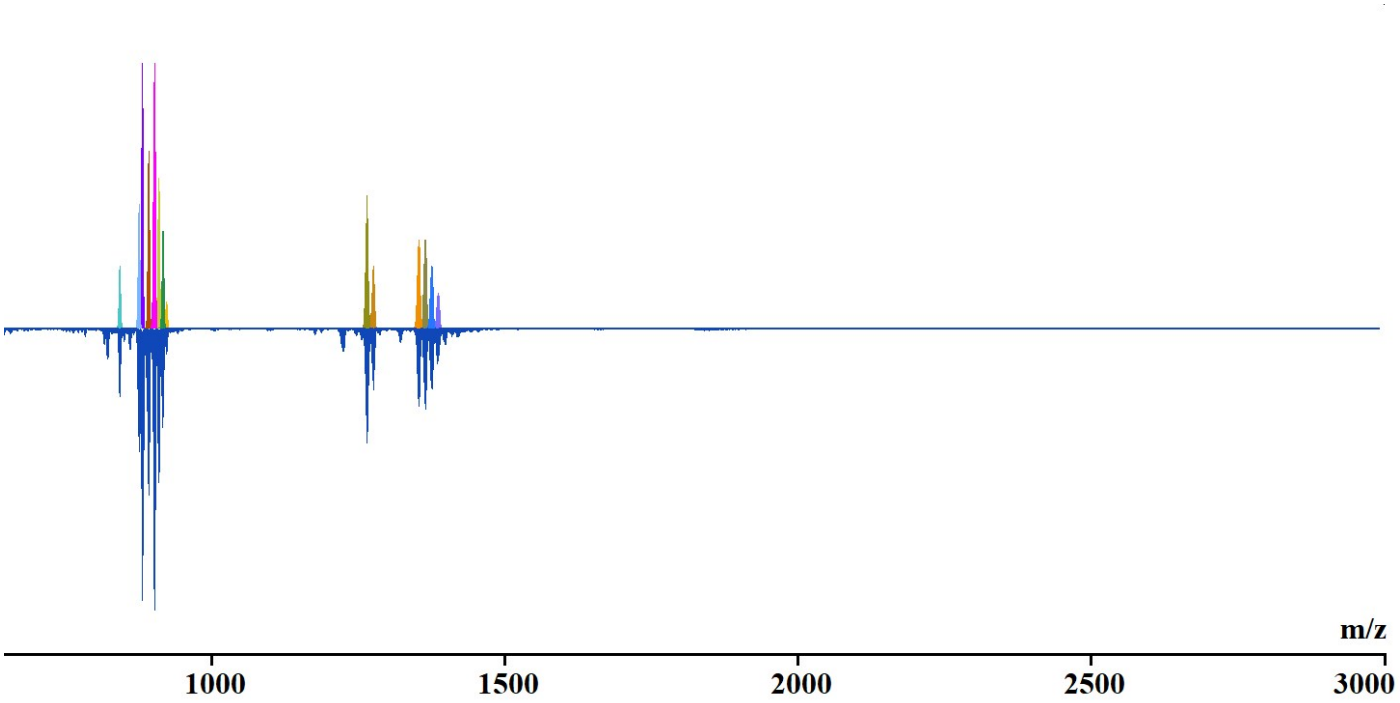

b) Zoomed area (840-895 m/z)

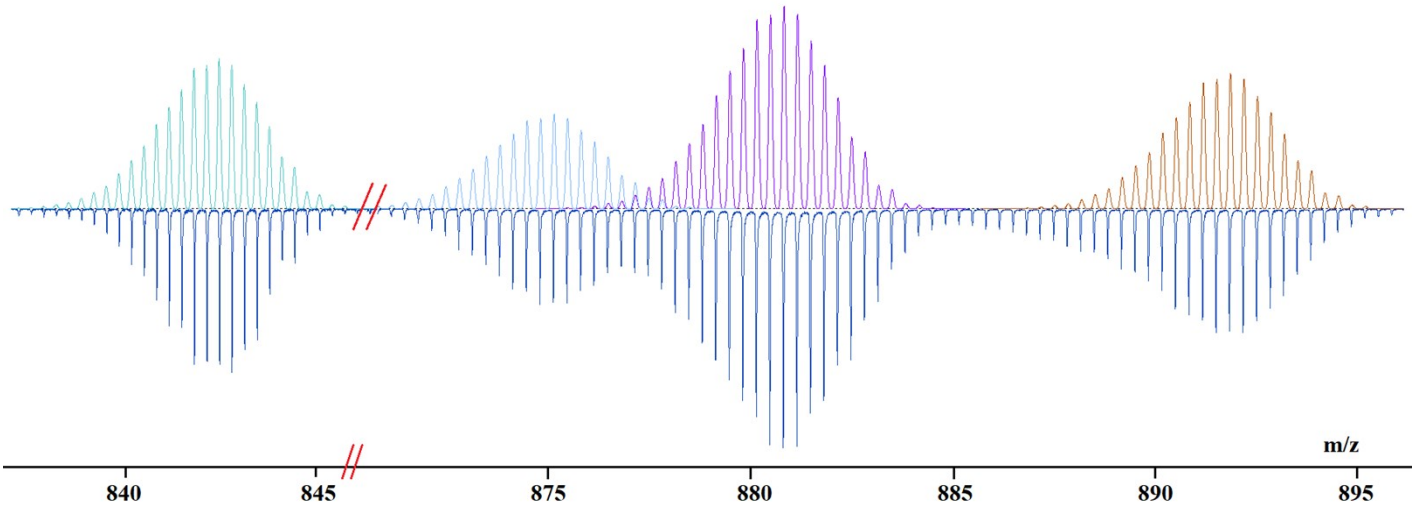

c) Zoomed area (900-925 m/z)

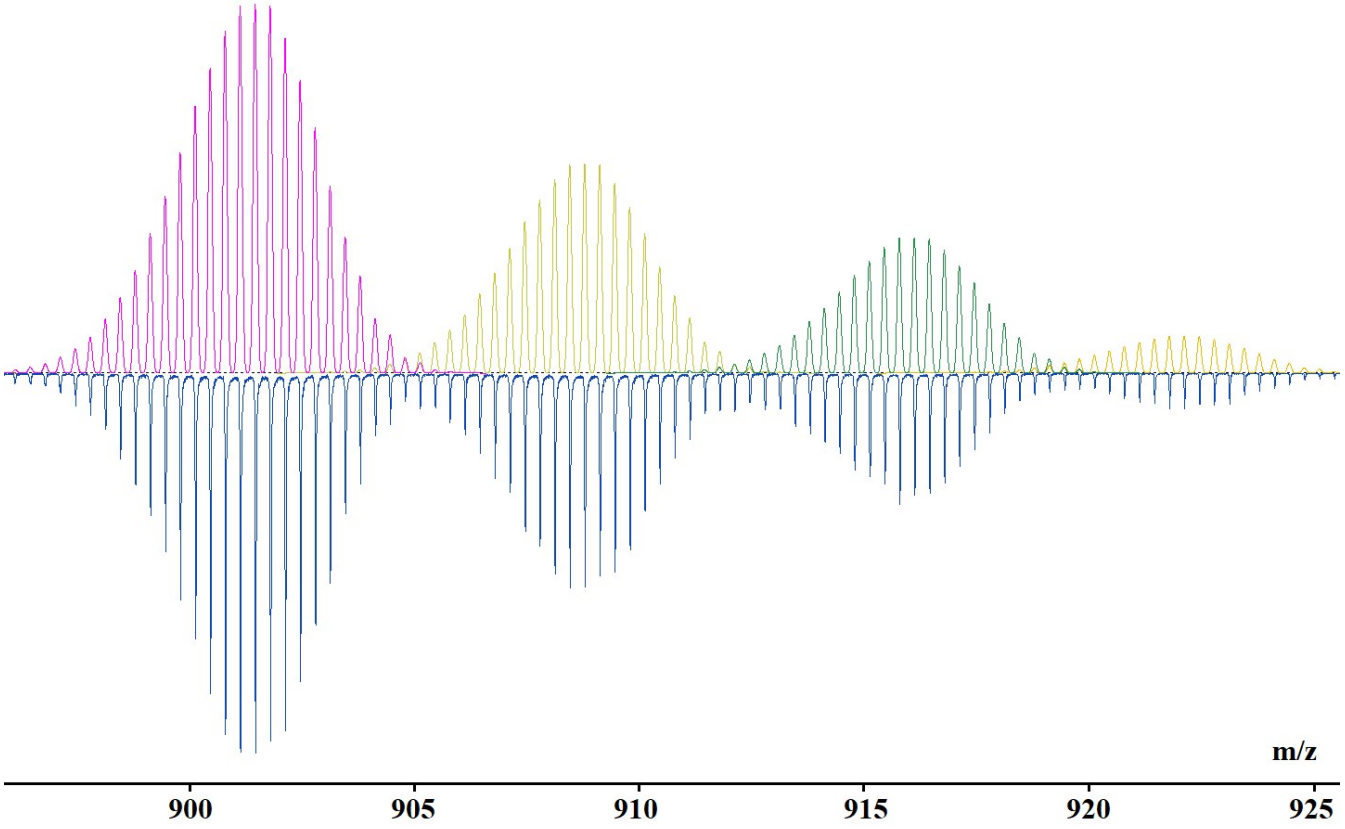

d) Zoomed area (1260-1280 m/z)

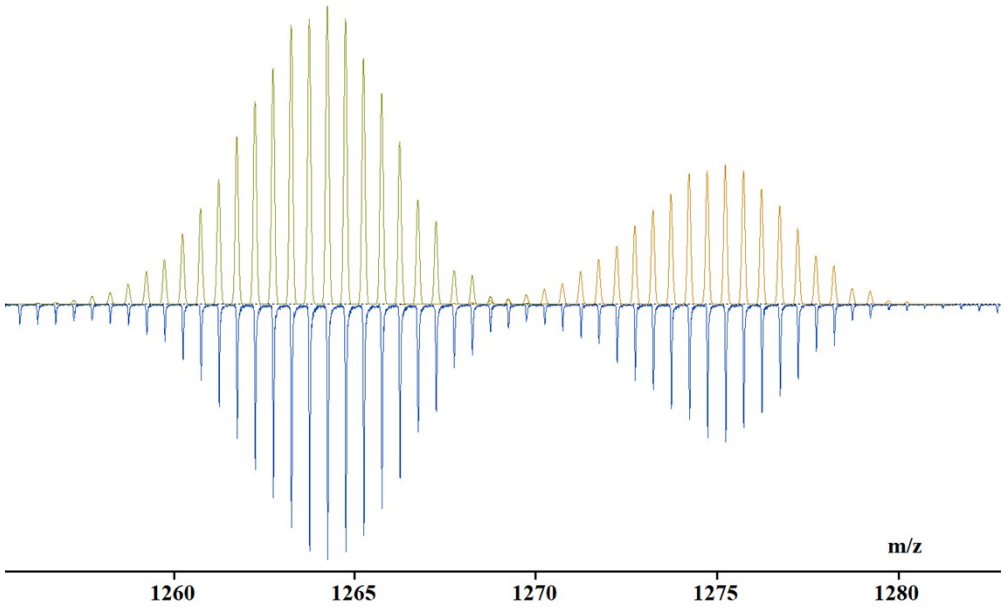

e) Zoomed area (1345-1390 m/z)

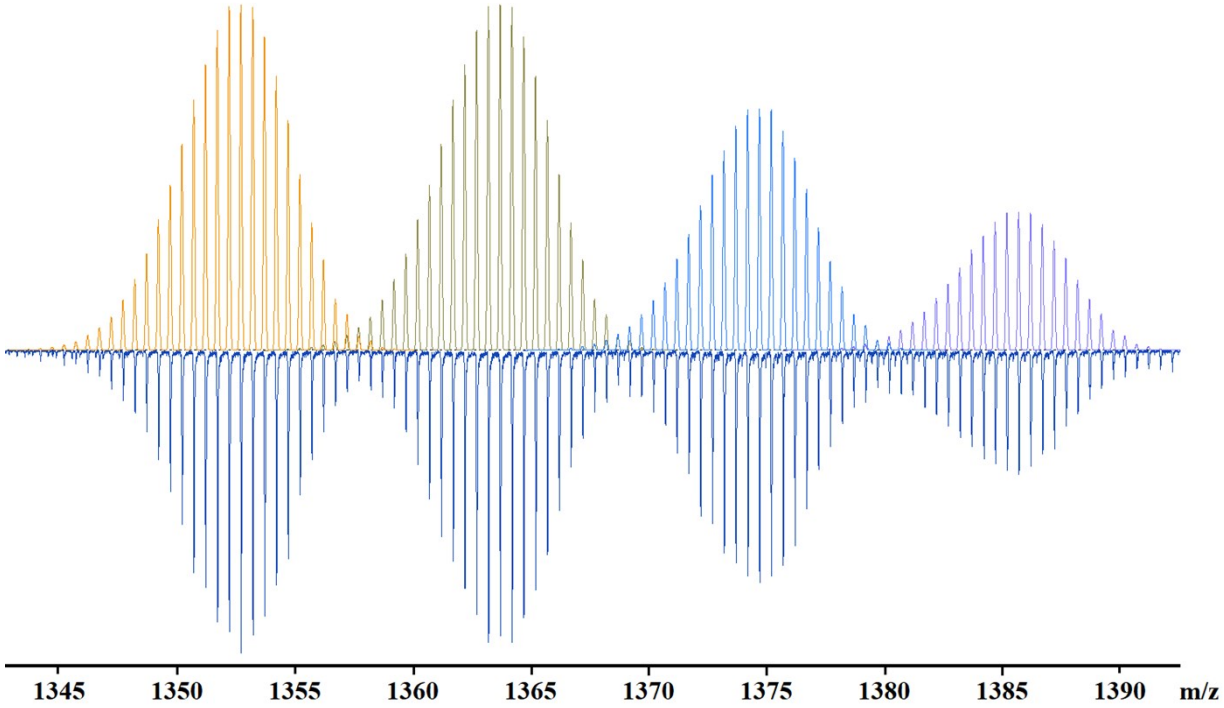

Table S6. HR-ESI-MS peak assignments of $Na_5[\{(C_6H_6)Ru\}_5VNb_{12}O_{40}]\cdot 16H_2O$ aqueous solution

Anion	**m/z exp**	**m/z calc**
$\{H_4VNb_{12}O_{40}(RuC_6H_6)_4\}^{3-}$	842.19	842.18
$\{Na_3HVNb_{12}O_{40}(RuC_6H_6)_4(CH_3OH)\}^{3-}$	874.82	874.84
$\{Na_3HVNb_{12}O_{40}(RuC_6H_6)_4(CH_3OH)(H_2O)\}^{3-}$	880.49	880.51
$\{Na_4VNb_{12}O_{40}(RuC_6H_6)_4(i\text{-}PrOH)\}^{3-}$	891.50	891.52
$\{H_2VNb_{12}O_{40}(RuC_6H_6)_5\}^{3-}$	901.24	901.23
$\{NaHVNb_{12}O_{40}(RuC_6H_6)_5\}^{3-}$	908.55	908.56
$\{Na_2VNb_{12}O_{40}(RuC_6H_6)_5\}^{3-}$	915.86	915.89
$\{Na_2VNb_{12}O_{40}(RuC_6H_6)_5(H_2O)\}^{3-}$	921.90	921.89
$\{H_5VNb_{12}O_{40}(RuC_6H_6)_4\}^{2-}$	1263.78	1263.77
$\{NaH_4VNb_{12}O_{40}(RuC_6H_6)_4\}^{2-}$	1274.77	1274.76
$\{H_3VNb_{12}O_{40}(RuC_6H_6)_5\}^{2-}$	1352.37	1352.35
$\{NaH_2VNb_{12}O_{40}(RuC_6H_6)_5\}^{2-}$	1363.35	1363.34
$\{Na_2HVNb_{12}O_{40}(RuC_6H_6)_5\}^{2-}$	1374.35	1374.33
$\{Na_3VNb_{12}O_{40}(RuC_6H_6)_5\}^{2-}$	1385.34	1385.32